

# Searches for lepton-flavour violation in $\tau$ decays at Belle and Belle II

---

Wenzhe Li<sup>a,\*</sup> on behalf of the Belle and Belle II collaborations

<sup>a</sup>Beihang University,  
Beijing 102206, Peoples's Republic of China

E-mail: [liwenzhe@buaa.edu.cn](mailto:liwenzhe@buaa.edu.cn)

The Belle II experiment is an upgrade of the Belle experiment, and both have extensive plans to search for new physics, in particular to search for lepton flavour and number and baryon number violations (LFV, LNV and BNV) in tau decays. In the low background environment of the  $e^+e^-$  collision experiment, the production cross section for  $\tau$  pairs is relatively large, providing many opportunities to search for  $\tau$  LFV decays in the Belle and Belle II experiments. We present recent results from the search for LFV decay  $\tau^- \rightarrow \ell^- V^0$  ( $\ell = e, \mu$  and  $V^0 = \rho^0, \omega, \phi, K^{*0}$  and  $\bar{K}^{*0}$ ) at Belle, and search for BNV decays  $\tau^- \rightarrow \Lambda\pi^-$  and  $\tau^- \rightarrow \bar{\Lambda}\pi^-$ , and LFV decay  $\tau^- \rightarrow \mu^-\mu^+\mu^-$  at Belle II.

42nd International Conference on High Energy Physics (ICHEP2024)  
18-24 July 2024  
Prague, Czech Republic

---

\*Speaker

## 1. Introduction

**Lepton** flavour violation (LFV) has long been recognised as a unambiguous signature of New Physics. LFV is allowed in various extensions of the Standard Model (SM), but has never been observed. **Fig. 1 shows the branching fraction upper limits (ULs)** at the 90% confidence level (CL) for existing LFV tau decays and what they are expected to be in the Belle II experiment. The following benchmark tau decays encompass almost all of the possible decay modes in the search for LFVs, including radiative decays  $\tau^- \rightarrow \ell^- \gamma$  ( $\ell = e, \mu$ ), leptonic decays  $\tau^- \rightarrow \ell^- \ell^+ \ell^-$ , semi-leptonic decays  $\tau^- \rightarrow \ell^- + \text{hadrons}$  and baryon number violation (BNV) decays  $\tau^- \rightarrow p \ell^- \ell^-$ ,  $\tau^- \rightarrow \Lambda \pi^-$ , and  $\tau^- \rightarrow \bar{\Lambda} \pi^-$ .

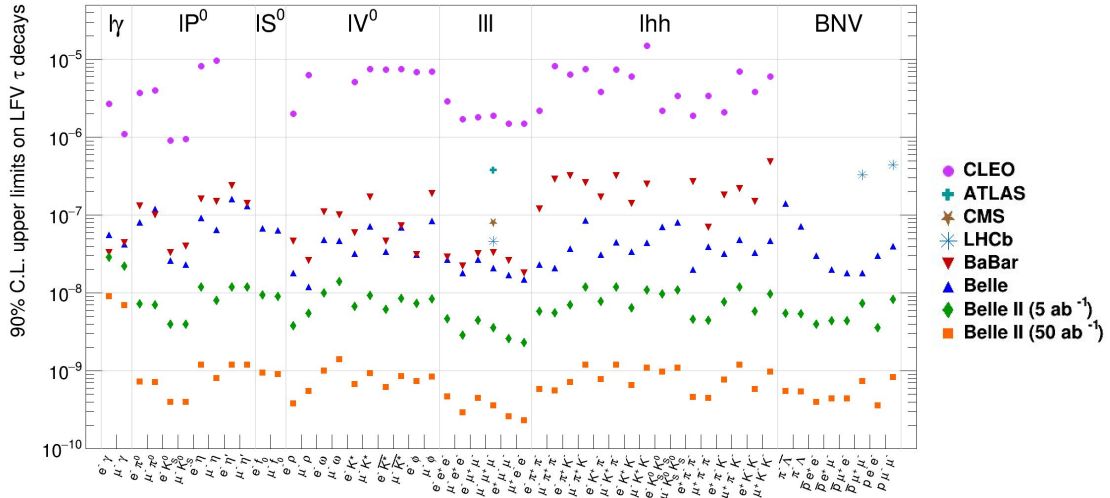


**Figure 1:** Current status of observed ULs at CLEO, BaBar, Belle, ATLAS, CMS, and LHCb experiments and the expected upper limits at the Belle II experiment [1].

Belle [2] operates at the KEKB asymmetric  $e^+e^-$  collider [3] in Tsukuba, Japan, and Belle II [4] and SuperKEKB [5] are upgrades of Belle and KEKB. In  $B$  factories such as Belle and Belle II, asymmetric energies  $e^+e^-$  collide at and near the  $\Upsilon(4S)$  **resonance**, and the cross section for  $B\bar{B}$  pairs and  $\tau$  pairs production is of the same order of magnitude, so they are also said to be  $\tau$  factories. When searching for LFVs in Belle and Belle II, our advantages include the known initial state, the clean environment, the high trigger **efficiency** and close to zero background searches. There is also the increase of the luminosity, with  $980 \text{ fb}^{-1}$  of data collected in Belle and  $530 \text{ fb}^{-1}$  in Belle II. Such a large data sample gives us more **sensitivity** to search for LFV tau decays.

We present several searches for decay channels that are forbidden in the SM but allowed in several new **physics** scenarios. For the LFV decay  $\tau^- \rightarrow \ell^- V^0$  ( $\ell = e, \mu$  and  $V^0 = \rho^0, \omega, \phi, K^{*0}$  and  $\bar{K}^{*0}$ ), we are most interested in the  $\tau^- \rightarrow \mu^- \phi$  mode, as it is a sensitive probe for leptoquark models. For BNV decay  $\tau^- \rightarrow \Lambda(\bar{\Lambda})\pi^-$ , BNV is one of the necessary conditions to explain the asymmetry of matter and antimatter and BNV is allowed in the beyond SM scenario. For LFV decay  $\tau^- \rightarrow \mu^- \mu^+ \mu^-$ , **it is experimentally the most accessible**.

## 2. Search for LFV decay $\tau^- \rightarrow \ell^- V^0$ at Belle

Previously, Belle performed this analysis using  $854 \text{ fb}^{-1}$  data and the **1-prong** tag method, **setting** the UL on the branching fractions at the 90% CL in the range of  $(1.2 \sim 8.4) \times 10^{-8}$  [6].

The latest results use the full Belle data at  $980 \text{ fb}^{-1}$ , add the 3-prong tag method, use Boost Decision Tree (BDT) to further suppress backgrounds [7]. Figs. 2(a) and 2(b) show the  $M_{\ell V^0}$  vs.  $\Delta E$  2D distributions for  $\tau^- \rightarrow e^- \phi$  and  $\tau^- \rightarrow \mu^- \phi$ , where  $M_{\ell V^0} = \sqrt{E_{\ell V^0}^2 - P_{\ell V^0}^2}$  is the invariant mass of the  $\ell V^0$  final state and  $\Delta E = E_{\ell V^0}^{\text{CM}} - \sqrt{s}/2$ . Here and following all equations,  $E$  and  $P$  indicate energy and momentum, respectively, the CM indicates the centre-of-mass system, and the  $\sqrt{s}$  is the centre-of-mass energy.

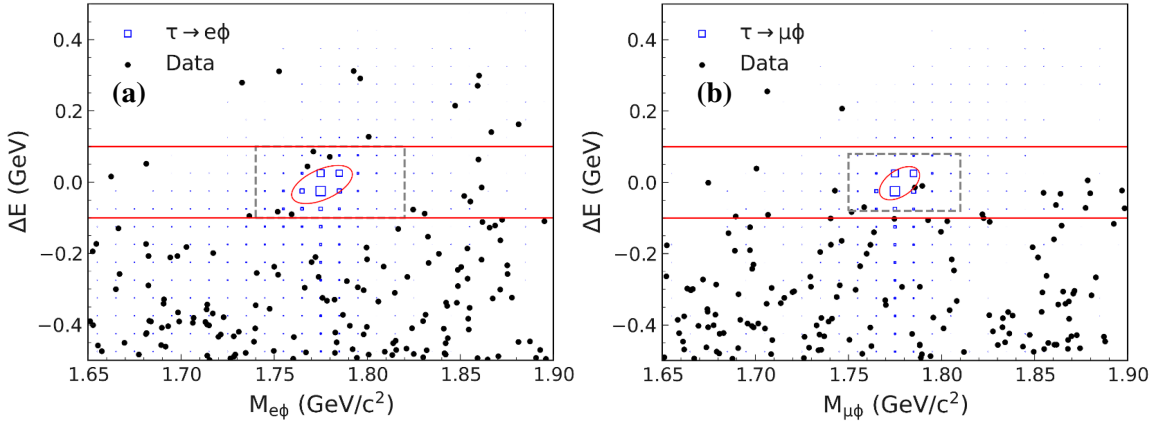


**Figure 2:** Distributions of selected events in the  $(M_{\ell V^0}, \Delta E)$  plane for (a)  $\tau^- \rightarrow e^- \phi$  and (b)  $\tau^- \rightarrow \mu^- \phi$ . The red elliptical lines are the signal regions. The gray dashed rectangles are the blind regions.

The estimations of the number of background events ( $N_{\text{BG}}$ ) are done using the data between the red horizontal lines outside the blind regions. The observed number of events ( $N_{\text{obs}}$ ) in the signal region (SR) has no excess over  $N_{\text{BG}}$ . The ULs at 90% CL on the branching fractions are listed in Table 1. With the 9% increase in signal efficiency and the  $126 \text{ fb}^{-1}$  additional data set, we achieved an average 30% improvement over previous results.

The results for  $\mathcal{B}(\tau^\pm \rightarrow \ell^\pm \rho^0)$  in Table 1 are worse compared to the previous results: for  $\tau^\pm \rightarrow \mu^\pm \rho^0$  channel, the Bayesian limits are used instead of the Frequentist limits, which are negatively proportional to  $N_{\text{BG}}$  when  $N_{\text{obs}}$  is fixed; for  $\tau^\pm \rightarrow e^\pm \rho^0$  channel, after unblinding, one event is observed in the signal region and the  $N_{\text{BG}}$  is greater than previously expected. The rest of the modes have achieved better limits than previously.

## 3. Search for BNV decays $\tau^- \rightarrow \Lambda(\bar{\Lambda})\pi^-$ at Belle II

The  $\tau^- \rightarrow \Lambda(\bar{\Lambda})\pi^-$  is a BNV decay as well as an LFV decay. Previously, Belle searched for this decay mode using  $154 \text{ fb}^{-1}$  of data and the 1-prong tag method, setting the UL on the branching fraction at 90% CL of  $0.72(1.4) \times 10^{-7}$  for  $\tau^- \rightarrow \Lambda(\bar{\Lambda})\pi^-$  decay mode [8].

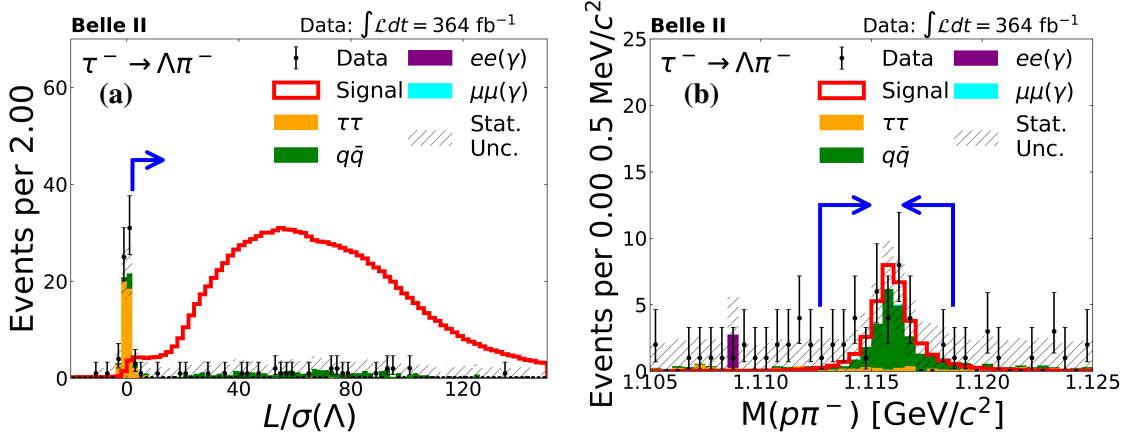
We searched for this decay mode using the  $364 \text{ fb}^{-1}$  data at Belle II [9], and we similarly reconstructed the four charged tracks using the 1-prong tag method, where  $\Lambda(\bar{\Lambda})$  is reconstructed

Mode	$N_{\text{BG}}$	$N_{\text{obs}}$	$\mathcal{B}_{\text{obs}}(\times 10^{-8})$
$\tau^\pm \rightarrow \mu^\pm \rho^0$	$0.95 \pm 0.20(\text{stat.}) \pm 0.15(\text{syst.})$	0	<1.7
$\tau^\pm \rightarrow e^\pm \rho^0$	$0.80 \pm 0.27(\text{stat.}) \pm 0.04(\text{syst.})$	1	<2.2
$\tau^\pm \rightarrow \mu^\pm \phi$	$0.47 \pm 0.15(\text{stat.}) \pm 0.05(\text{syst.})$	0	<2.3
$\tau^\pm \rightarrow e^\pm \phi$	$0.38 \pm 0.21(\text{stat.}) \pm 0.00(\text{syst.})$	0	<2.0
$\tau^\pm \rightarrow \mu^\pm \omega$	$0.32 \pm 0.23(\text{stat.}) \pm 0.19(\text{syst.})$	0	<3.9
$\tau^\pm \rightarrow e^\pm \omega$	$0.74 \pm 0.43(\text{stat.}) \pm 0.06(\text{syst.})$	0	<2.4
$\tau^\pm \rightarrow \mu^\pm K^{*0}$	$0.84 \pm 0.25(\text{stat.}) \pm 0.31(\text{syst.})$	0	<2.9
$\tau^\pm \rightarrow e^\pm K^{*0}$	$0.54 \pm 0.21(\text{stat.}) \pm 0.16(\text{syst.})$	0	<1.9
$\tau^\pm \rightarrow \mu^\pm \bar{K}^{*0}$	$0.58 \pm 0.17(\text{stat.}) \pm 0.12(\text{syst.})$	1	<4.3
$\tau^\pm \rightarrow e^\pm \bar{K}^{*0}$	$0.25 \pm 0.11(\text{stat.}) \pm 0.02(\text{syst.})$	0	<1.7

**Table 1:** Summary of the ULs on  $\mathcal{B}(\tau \rightarrow \ell V^0)$ .

from a  $p(\bar{p})$  and  $\pi^-(\pi^+)$ , and for the signal selection and background suppression we used loose pre-selection, followed by Gradient-BDT (GBDT). Figs. 3(a) shows the flight significance (the flight distance  $L$  divided by its uncertainty  $\sigma$ ) of  $\Lambda$  candidates, it is one of the most discriminant variables, and a large number of backgrounds are excluded using this variable during the pre-selection stage.

The resulting  $p\pi^-$  invariant mass distribution is shown in Fig. 3(b). Figs. 4(a) and 4(b) show the  $M(\Lambda\pi)$  vs.  $\Delta E$  2D distributions for  $\tau^- \rightarrow \Lambda\pi^-$  and  $\tau^- \rightarrow \bar{\Lambda}\pi^-$ , where  $M(\Lambda\pi) = \sqrt{E_{\Lambda\pi}^2 - P_{\Lambda\pi}^2}$  and  $\Delta E = E_{\Lambda\pi}^{\text{CM}} - \sqrt{s}/2$ .

**Figure 3:** Distributions of (a)  $L/\sigma$  and (b)  $M(p\pi^-)$  of  $\Lambda$  candidates for  $\tau^- \rightarrow \Lambda\pi^-$ .

We used the Poisson counting experimental technique to calculate the expected number of events within the **sideband** regions. The expected number of events is 1 (0.5) for  $\tau^- \rightarrow \Lambda(\bar{\Lambda}\pi^-)$  channel. The signal efficiency is 9.5% (9.9%) for  $\tau^- \rightarrow \Lambda(\bar{\Lambda}\pi^-)$  channel. No events are observed within the SR for both decay modes, so we use the Bayesian approach to estimate the UL on the branching fraction at 90% CL of  $4.7(4.3) \times 10^{-8}$  for  $\tau^- \rightarrow \Lambda(\bar{\Lambda}\pi^-)$  channel.

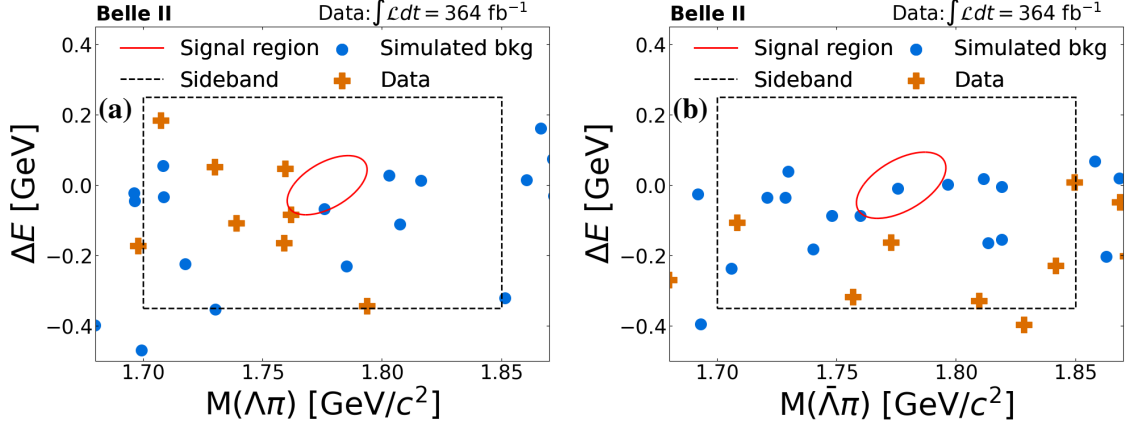


**Figure 4:** Distributions of selected events in the  $(M(\Lambda\pi), \Delta E)$  plane for (a)  $\tau^- \rightarrow \Lambda\pi^-$  and (b)  $\tau^- \rightarrow \bar{\Lambda}\pi^-$  channels. The red solid ellipses identify the SRs, while the areas between the dashed black boxes and the corresponding ellipses are the sideband regions.

#### 4. Search for LFV decay $\tau^- \rightarrow \mu^- \mu^+ \mu^-$ at Belle II

Previously, Belle searched for this decay mode using  $782 \text{ fb}^{-1}$  of data and the 1-prong tag method, setting the UL on the branching fraction at 90% CL of  $2.1 \times 10^{-8}$  for  $\tau^- \rightarrow \mu^- \mu^+ \mu^-$  decay mode [10].

We use the inclusive tag method based on  $424 \text{ fb}^{-1}$  data at Belle II to search for this decay mode and use the BDT method to further suppress the background [11]. Fig. 5(a) shows the  $M_{3\mu}$  vs.  $\Delta E_{3\mu}$  2D distributions for  $\tau^- \rightarrow \mu^- \mu^+ \mu^-$  channel, where  $M_{3\mu} = \sqrt{E_{3\mu}^2 - P_{3\mu}^2}$  and  $\Delta E_{3\mu} = E_{3\mu}^{\text{CM}} - \sqrt{s}/2$ . For a real  $\tau^- \rightarrow \mu^- \mu^+ \mu^-$  signal event,  $\Delta E_{3\mu}$  should be near 0 and  $M_{3\mu}$  should be near the normal  $\tau$  mass. The radiation of photons from the initial state leads to a tail at low values of  $\Delta E_{3\mu}$ . Instead, final state radiation produces a tail at high values of  $M_{3\mu}$  and  $\Delta E_{3\mu}$ .

Using a novel inclusive-tagging reconstruction followed by a BDT-based selection, the efficiency is higher by a factor of 2.5 than the efficiency in the latest Belle analysis. Fig. 5(b) shows the CLs curves computed as a function of the UL on the branching fractions for the inclusive tagging analysis. The dashed black line shows the expected CLs and the green and yellow bands give the  $\pm 1\sigma$  and  $\pm 2\sigma$  contours, respectively. The expected number of background events is 0.7 and one event observed in the SR. The observed (expected) UL at 90% C.L. computed in a frequentist approach is  $1.9 (1.8) \times 10^{-8}$ , which is more restrictive than the previous results.

#### 5. Conclusion

The Belle(II) detector provides significant advantages for searching for LFV in tau decays, including increased luminosity, and improved **detection efficiency**. In the  $\tau^- \rightarrow \ell^- V^0$ ,  $\tau^- \rightarrow \Lambda(\bar{\Lambda}\pi^-)$ , and  $\tau^- \rightarrow \mu^- \mu^+ \mu^-$  analyses presented above, we achieved higher signal efficiencies and lower background levels using either larger data samples than previously, or more advanced analysis techniques (tagging and BDT) than previously. In these analyses, with the exception of the  $\tau^\pm \rightarrow \ell^\pm \rho^0$  model, we estimate by far the tightest the limits on the branching fractions in the

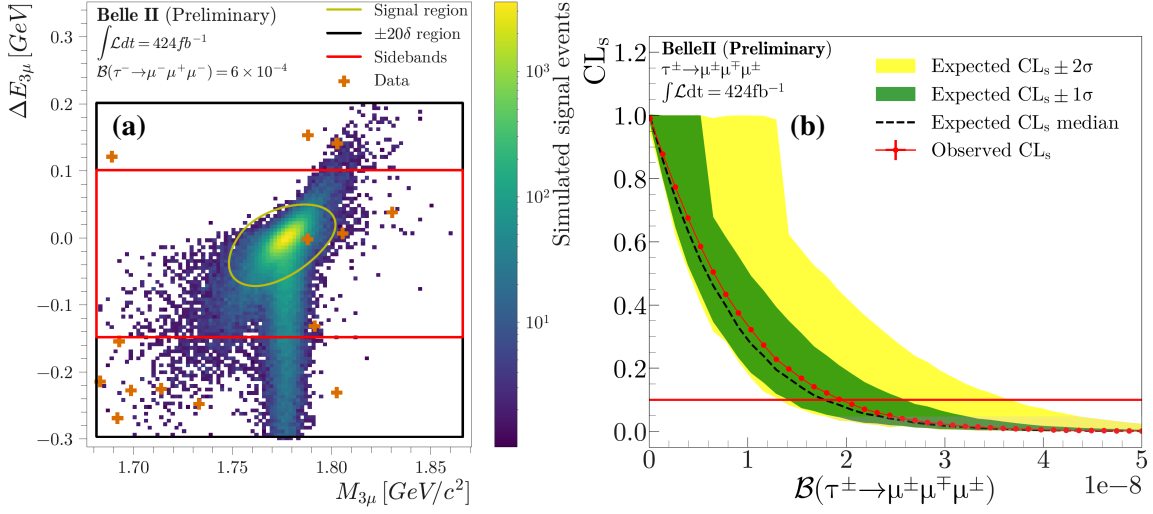


**Figure 5:** Distributions of (a) the selected events in the  $(M_{3\mu}, \Delta E_{3\mu})$  plane and (b) the observed and expected CL as a function of the assumed branching fraction of  $\tau^- \rightarrow \mu^- \mu^+ \mu^-$ .

world. As Belle II data continues to be collected, we believe that more world-leading results are on the way.

## References

- [1] S. Banerjee *et al.*, [arXiv:2203.14919](#) (2022).
- [2] A. Abashian *et al.* (Belle Collaboration), *Nucl. Instrum. Meth. A* **479**, 117 (2002).
- [3] S. Kurokawa and E. Kikutani, *Nucl. Instrum. Meth. A* **499**, 1 (2003). T. Abe *et al.*, *Prog. Theor. Exp. Phys.* **2013**, 3 (2013).
- [4] T. Abe *et al.* (Belle II Collaboration), [arXiv:1011.0352](#) (2010).
- [5] K. Akai, K. Furukawa, and H. Koiso, *Nucl. Instrum. Meth. A* **907**, 188 (2018).
- [6] Y. Miyazaki *et al.* (Belle collaboration), *Phys. Lett. B* **699**, 251 (2011).
- [7] N. Tsuzuki *et al.* (Belle II collaboration), *JHEP* **2023**, 118 (2023).
- [8] Y. Miyazaki *et al.* (Belle collaboration), *Phys. Lett. B* **632**, 51 (2006).
- [9] I. Adachi *et al.* (Belle II collaboration), [arXiv:2407.05117](#) (2024).
- [10] K. Hayasaka *et al.* (Belle collaboration), *Phys. Lett. B* **687**, 139 (2010).
- [11] I. Adachi *et al.* (Belle II collaboration), [arXiv:2405.07386](#) (2024).